J Mater Sci: Mater Med (2010) 21:2491–2500
DOI 10.1007/s10856-010-4092-7

PVA/STMP based hydrogels as potential substitutes of human vitreous

Gemma Leone · Marco Consumi · Marianna Aggravi · Alessandro Donati · Stefania Lamponi · Agnese Magnani

Received: 12 February 2010 / Accepted: 3 May 2010 / Published online: 25 May 2010

Abstract PVA based hydrogels were synthesised using, as crosslinking agent, trisodium trimetaphosphate (STMP) to obtain potential substitutes for the vitreous body of the eye. The hydrogels, obtained using different amounts of STMP, were characterised by Infrared Spectroscopy which confirmed the successful occurrence of crosslinking reaction. The mechanical spectra of the fully hydrated samples confirmed covalently crosslinked systems (i.e. $G' > G''$). The rheological analysis pointed out that only one of the hydrogels (PVA STMP 8:1) showed a behaviour similar to that of human vitreous. The hydrogel was also subjected to injection through a small needle, a procedure that is essential in the use of vitreous substitutes. Further analysis in terms of light transmittance, water content measurements, diffusion coefficient and cytotoxicity confirmed the applicability of such a hydrogel as vitreous substitute.

1 Introduction

The vitreous body is a clear and transparent jellylike mass comprised of a network of protein fibrils (i.e. collagen type II) and hyaluronan. However, the network component represents only a small fraction of its mass (i.e. 1%), the remaining 99% is represented by water. The vitreous fills the posterior cavity of the eye and occupies more than two-thirds of the ocular volume. It provides an adequate support for the retina, protects the surrounding ocular tissues from adverse circumstances, allows light to reach the sensory elements at the back of the eye, and metabolic solutes to diffuse [1].

The surgical treatment of various complicated retinal detachments requires the availability of a vitreous substitute, either temporary or permanent, ideally to be injectable into the vitreous cavity at the time of surgery. The purpose of injecting a fluid into the vitreous cavity is the restoration of the volume and internal pressure of the ocular globe, because the natural vitreous usually collapses during surgical intervention. The injected material should be able to exert a hydraulic pressure so as to provide tamponade to the retina against the choroid, and also to alter the characteristics of the vitreous in order to relax and prevent vitreoretinal tractions [2].

Sodium hyaluronate and other polysaccharides, such as dextran, alginic acid, chondroitin sulfate, guar gum, methylcellulose, carboxymethylcellulose and hydroxypropylmethylcellulose (HPMC), were studied as vitreous substitutes [3, 4]. Water-soluble high molecular weight polymers have rheologic properties that permit the highly viscous solutions to be injected in the eye through small gauge needles. These viscoelastic polymer solutions can help reattach the retina when it is forced by injection against the detached retina. In addition, their high viscosity may retard the flow of the solution through a retinal break while subretinal fluid is being drained intraoperatively.

Nevertheless, the main defect of all these products is their short residence time in eye cavity. In fact, they are re-absorbed in relatively short periods of time.

Actually, silicone oil is the most commonly used temporary vitreous substitute [5]. Silicone oil is an effective long term retinal tamponade. When silicone oil is injected into the vitreous, it remains in the eye until it is surgically removed. However, the ability of the eye to tolerate this foreign material has been repeatedly questioned. Different

G. Leone (✉) · M. Consumi · M. Aggravi · A. Donati · S. Lamponi · A. Magnani
Department of Pharmaceutical and Applied Chemistry, University of Siena, Via Aldo Moro 2, 53100 Siena, Italy
e-mail: leone10@unisi.it

formulation, over the last decades, have been realised but all of them can induce complications such as disappearance of the outer plexiform layer and disorganization of the photo-receptor layer in eyes subjected to the treatment with silicon oils [6, 7]. Some of the studies have found that silicone oil may infiltrate various tissues of the eye [8, 9]. Since the 1980s, studies have reported the impregnation of the optic nerve with what was presumed to be silicone oil, both in front of and behind the lamina cribrosa [10, 11]. Furthermore, intraocular silicone oil, under special circumstances, may migrate into the brain through the subarachnoidal space [12]. However, the most frequent event is the formation of a emulsification within the eye due to the infiltration of humour aqueous into the eye cavity containing the silicon oil [13].

A hydrogel being formed for over 90% by water should drastically decrease the risk of the emulsification once implanted into the eye cavity.

In this work a new poly(vinyl-alcohol) (PVA) based hydrogel as potential vitreous substitute was realised. The choice of PVA was due to its good performance in ophthalmologic application [14].

A new method to crosslink PVA, based on the use of a non toxic substance as crosslinking agent, trisodium trimetaphosphate (STMP), used to crosslink starch in the food industry, was proposed [15]. Several molar ratios between STMP and PVA were realised. Rheological analysis was used as a criteria for choosing the most suitable vitreous substitute among the synthesised hydrogels. The best candidates were further characterised in terms of light transmittance and water uptake. Finally, cytotoxicity was assessed by in vitro test.

2 Materials and methods

2.1 Materials

All materials and reagents were purchased from Fluka Sigma–Aldrich (Switzerland). All used solvents were of analytical or HPLC grades.

2.2 Methods

2.2.1 PVA crosslinking

A 5% (w/v) solution of PVA was prepared in basified water (pH 12, with NaOH 2 M). Poly-vinyl alcohol (PVA) was crosslinked with different amounts of trisodium trimetaphosphate (STMP). Samples with five different STMP/PVA molar ratios were realised (STMP/PVA: 1:1; 1:2; 1:4; 1:6 and 1:8). The reaction mixtures were stirred for 2 h, maintaining the pH 12 by the addition of 2 M NaOH, at 70°C. The obtained hydrogels (PVA_cr1; PVA_cr2; PVA_cr4; PVA_cr6; PVA_cr8) were then poured into petri dishes and dried at RT for 18 h. The obtained soft films were rinsed with large volumes of distilled water and further dried until no weight loss could be detected.

2.2.2 Characterization

2.2.2.1 Infrared analysis ATR spectra of native and crosslinked PVA in dry form were recorded on a Nicolet Thermo 7000 apparatus between 4000 and 750 cm^{-1} wavenumbers. A MCT (Mercury–Cadmium–Tellurium) detector was used, and the apparatus was purged with nitrogen. Typically, 64 scans at a resolution of 1.0 cm^{-1} were averaged. The frequency scale was internally calibrated with a helium–neon reference laser to an accuracy of 0.01 cm^{-1}.

2.2.2.2 Rheological measurements A controlled strain rheometer (AR2000, TA Instruments, Leatherhead, United Kingdom) was used for all rheological measurements (strain sweep analysis, oscillatory shear stress analysis and shear creep analysis) which were performed at 37°C. Fully hydrated samples (NaCl 0.9%) of approximately 1.2 ml each are placed between a 60-mm diameter lower plate and a 4″/40-mm diameter cone truncated to give a gap of 0.15 mm. Smooth and rigid circular plates were used for testing. The plates are impermeable to fluid flow to reduce the free surface of the sample and minimize dehydration during testing.

Strain sweep tests, consisting in monitoring the viscoelastic properties while logarithmically varying the strain amplitude $\gamma 0$, at a fixed oscillation frequency (0.007, 1 and 5 Hz) were performed on the materials to determine the strain amplitude at which linear viscoelasticity is valid.

Oscillatory shear stress analysis. Oscillatory shear experiments and the resulting plots of real (G′, the storage modulus) and imaginary (G″, the loss modulus) parts of the complex dynamic shear modulus versus the frequency of oscillatory stress, sometimes termed as mechanical spectra, are currently used to demonstrates the gel character, and to discriminate between different classes of gels such as entanglements networks or covalently crosslinked gels [16]. The oscillatory test was used as a criteria for potential vitreous substitutes [17]. The mechanical properties of PVA based hydrogels were studied by analysing the storage (G′), the loss (G″) modulus as a function of frequency. Since sufficient resilience of the material, when subjected to shear stress, is also desirable for vitreous substitutes, this parameter was estimated by recording the dissipation factor, also known as the loss tangent. Resilience (R) is an inverse measure of the damping property and usually estimated as $R = 1 - 2\pi \tan \delta$ (where δ is the ratio

between G″ and G′) [18]. A material that behaves as a perfectly elastic solid has no energy dissipation and a stress in phase with the strain (i.e. $\delta = 0°$), whereas a perfectly viscous fluid has no energy storage and a stress and strain 90° out of phase.

For the dynamic shear tests, the samples were subjected to a sinusoidal angular displacement. A dynamic frequency sweep test was performed with a shear amplitude of $\gamma 0 = 0.01$ rad over the frequency range 0.007–5 Hz [17, 19].

Shear creep analysis. In a shear creep experiment a constant shear stress (σ_0) is imposed for a specified time. In viscoelastic materials the strain response is linear. The ratio $\gamma t/\sigma_0$, where γ is the strain, is called shear creep compliance J(t).

A shear stress of 0.1 Pa was applied to the gel samples with a nominal creep time of 500 s [2].

All the samples were analysed with the exception of PVAcr_1 which was too hard to be analysed by a rheometer.

The same analysis was performed on a commercial silicon oil used as temporary vitreous substitute.

2.2.2.3 Kinetics of hydration and water uptake A known amount of each sample (5 mg) was positioned on a cell-culture strainer and immersed in NaCl 0.9% in a thermostatic bath at 37°C. The weight of the sample was monitored until it reached the swelling equilibrium and determined using the formula (1):

$$\text{W.U.} = (W_s - W_d/W_d) \times 100 \quad (1)$$

The water content of the hydrogel was determined using the formula (2):

$$\text{W.C.} = (W_s - W_d/W_s) \times 100 \quad (2)$$

where the W_s and W_d are the weight of swollen and dried hydrogel, respectively.

2.2.2.4 Light transmittance The PVA based hydrogels were immersed in NaCl 0.9% at 25°C for swelling equilibrium, and then cut into rectangular membranes 1 cm × 1 cm in size. The membranes were adhered onto the surface of quartz cube cell, and the transmittance was measured using UV–vis Spectrophotomer (Perkin-Elmer Lamda 25) from 700 to 380 nm. Every membrane was measured for 5 scans [20].

2.2.2.5 In vitro cytotoxicity, cell proliferation and viability To evaluate the in vitro cytotoxicity of hydrogels, the direct contact test, proposed by "ISO 10993-5 Biological evaluation of medical devices—Part 5: Tests for cytotoxicity: in vitro methods", was utilised. This test is suitable for samples with various shapes, sizes or physical states (i.e. liquid or solid).

Mouse tumoral fibroblasts NIH3T3 were utilised for cytotoxicity, cell proliferation and viability experiments. Tumoral mouse NIH3T3 fibroblasts were propagated in Dulbecco's modified Eagle's medium (DMEM) with 10% fetal calf serum, 1% L-glutamine–penicillin–streptomycin solution, and 1% MEM Non-Essential Amino Acid Solution, at 37°C in a humidified atmosphere containing 5% CO_2. Once at confluence, cells were washed with PBS 1×, taken up with trypsin–EDTA solution and then centrifuged at 1000 rpm for 10 min. The pellet was re-suspended in complete DMEM solution (dilution 1:15).

Ten milligrams of each swollen hydrogel were sterilised with 70% EtOH for 1 h at room temperature. Then, EtOH was removed and samples washed by culture medium. High Density Polyethylene (HDPE, U.S. Pharmacopeia, Rockville-Maryland, USA) was used as negative control. All samples were set up in triplicate.

1.0×10^3 cells suspended in 1 ml of complete medium were seeded in each well of a 24 well round multidish and incubated at 37°C in an atmosphere of 5% CO_2 for 24 h. Then, the hydrogels were put on the adhered cells. In order to avoid the hydrogels floating, the samples were covered and fixed by a co-culture insert having a PET membrane with pores of Ø = 0.4 μm (Falcon, USA).

The number of cells in contact with hydrogels was evaluated by an inverted optical microscopy (IX 50, Olympus, Germany) at the following intervals: 24, 48 and 72 h. Cells were counted directly or by previous fixing in 2.5% glutaraldehyde in 100 mM sodium cacodylate and staining by toluidine blue. Images of cells in contact with hydrogels were captured by a digital camera applied to the microscopy (Camedia C5050, Olympus, Germany).

Cell viability after 24, 48 and 72 h of contact with different hydrogels was evaluated by WST-1 assay (Roche, Germany).The Cell Proliferation Reagent WST-1 is a ready-to-use substrate which measures the metabolic activity of viable cells. This colorimetric assay is based on the reduction of tetrazolium (WST-1) salts to coloured formazan compounds by living (metabolically active) cells. Tetrazolium salt (WST-1) is cleaved to soluble Formazan dye by mitochondria dehydrogenase, which is only active in viable cells. The increase of enzyme activity leads to an increase of the production of Formazan dye, so the quantity of Formazan dye measured by 450 nm absorbance is directly proportional to the living cells in culture. The procedure is rapid, accurate and can assay as low as 1000 cells/well (assay range is 1000 to 100,000 cells/well).

At intervals of 24 h the medium was removed from each well, the WST-1 was added and incubated at 37°C in 5% CO_2 for 3 h. At the end of incubation period, the WST-I was removed and the amount of formazan salt produced by viable cells was measured reading the absorbance at 450 nm by an ELISA plate reader (BIOTRAK II

Microplate Reader and Washer, Biochrom Ltd, UK). The absorbance was directly correlated to viable cell number by using a standard curve previously obtained.

Multiple comparison were performed by one-way ANOVA and individual differences tested by Fisher's test after the demonstration of significant intergroup differences by ANOVA. Differences with $P < 0.05$ were considered significant.

2.2.2.6 Thixotropic properties An artificial vitreous should be a viscoelastic material and should maintain this quality after injection through a small-gauge needle. A thixotropic material is able to become fluid in the presence of an appropriate mechanical stimulus whereas it resumes the original consistency with stimulus removal. The thixotropic behaviour of the hydrogels was assessed with a loop test using an AR2000 rheometer at 37°C. The G′ (storage modulus) and G″ (loss modulus) were recorded increasing the applied stress in logarithmic mode (ten points per decade; equilibration time for each measurement 60 s), from a minimum (0.0636 Pa) to a maximum (100 Pa) value. The applied stress was then decreased to the initial value, following the same procedure [21]. To confirm the injectability of the swollen hydrogel, it was placed inside a syringe and subjected to a mechanical stimulus consisting of the piston movement. It was necessary to repeat the piston movement two to three times to obtain a fluid compound. The fluid passed through a 19 gauge needle and resumed instantaneously the original hydrogel consistency. After injection through the 19 gauge needle the rheological characterisation was performed following the procedure previously reported.

2.2.2.7 Diffusion coefficient: NMR spectroscopy and data analysis Understanding the diffusion behaviour of an hydrogel is important for its applicability as vitreous substitute. The diffusion coefficient of a model solute, phenylalanine in D_2O and inside the hydrogel was determined by NMR. ^{1}H NMR spectra were obtained at 14.1 T with a Bruker Avance 600 Spectrometer operating at controlled temperature.

DOSY spectra were acquired at 310 K using a 5 mm SEI probe with gradients along z axis. A 2D sequence for diffusion measurement using stimulated echo using bipolar gradient pulses for diffusion using one spoil gradient was used [22]. Water suppression was achieved using 3–9–19 pulse sequence with gradients [23].

Diffusion coefficient were measured by incrementing the gradient strength (with an initial value of 0.71 G cm $^{-1}$ and a step size of 2.21 G cm^{-1} for 1.20 ms), while the separations (100 ms) of the fields gradients and the total echo time were kept constant. A series of 16 spectra with 8 scans were recorded in 2D mode for each measurements with a recycle time of 1 s between scans.

The strength of the B_0 field gradient was calibrated by measuring the self diffusion coefficient of the residual HDO signal in 100% D_2O sample at 298 K.

In order to determine the value of the diffusion constant the intensity of the aromatic protons of phenylalanine was plotted as function of the gradient strength G and regression analysis was performed by XWIN-NMR 3.5 software according to Eq. 3:

$$I = I_0 \exp[-D4\pi^2\gamma^2G^2\delta^2(\Delta - \delta/3)] \quad (3)$$

where D is the diffusion coefficient, γ is the giromagnetic ratio, G is the magnetic field-gradient strength, Δ is the time interval separating the gradient pulses (big delta: the effective diffusion interval) and δ (little delta) is the gradient pulse duration.

For isotropic diffusion, the self diffusion coefficient can be obtained by non linear fitting of the Eq. 3 to the data.

3 Results and discussion

3.1 Infrared analysis

Infrared spectra were recorded to confirm the crosslinking of PVA. In Fig. 1 the infrared spectra of native PVA and PVA_cr8 were reported and compared. The IR spectrum of PVA_cr1, PVA_cr2, PVA_cr4 and PVA_cr6 are not reported since they did not show significant differences with respect to PVA_cr8. The main wavenumbers observed in the IR spectra are summarised in Table 1 together with their assignments. The IR spectrum of native PVA (Fig. 1, black curve) shows typical inter and intramolecular bond OH stretching band at 3300 cm^{-1}, symmetric and

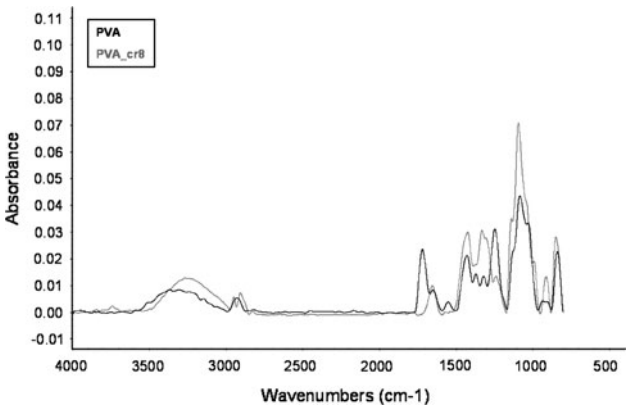

Fig. 1 IR spectra of native PVA (*black curve*) and crosslinked PVA_cr8 (*grey curve*). The PVA_cr8 spectrum showed two broad bands and new characteristic peaks and shoulders at 1299 cm^{-1} (pyrophosphate systems), 1131, 982 and 906 cm^{-1} (phosphate group)

Table 1 Main wavenumbers observed in the IR spectra of native PVA and PVA_cr8 together with their assignments

Sample	v (cm^{-1})	Assignments
PVA	3300	OH H-bonded
	2928	CH_2 asymmetric stretching
	2850	CH_2 symmetric stretching
	1720	COOR stretching
	1246	C–O stretching
PVA_cr8	3300	OH H-bonded
	2928	CH_2 asymmetric stretching
	2850	CH_2 symmetric stretching
	1299	P–O–P (pyrophosphate systems) stretching
	1131, 982, 906	PO_3^- stretching

asymmetric stretching bands relative to CH_2 moieties (2928 and 2850 cm^{-1}, respectively) and a peak centred at about 1720 cm^{-1} which can be attributed to the presence of the acetoxy group. In fact, PVA is currently produced mostly by the saponification of poly(viny1 acetate) with alkaline methanol or ethanol and it is characterised by the presence of residual acetoxy groups. Their percentage determines the solubility of PVA.

The IR spectrum of the PVA_cr8 (Fig. 1, grey curve) reveals a small band broadening with respect to that of PVA. This phenomenon is characteristic of crosslinked materials. Furthermore, significant peaks in the region 1307–1206 cm^{-1}, relative to pyrophosphate systems, appeared. In addition, the IR spectrum of PVA_cr8 showed two shoulders centred at 1131 and 982 cm^{-1} and one new peak centred at 906 cm^{-1} which are relative to phosphate group [24]. The disappearance of the peak centred at 1720 cm^{-1}, which is relative to the acetoxy group was due to the basified environment in which the reaction of crosslinking was carried out.

3.2 Rheological measurements

3.2.1 Oscillatory shear analysis

Representative mechanical spectra are shown in Fig. 2. The G′ and G″ values at 5 Hz relative to all the samples are reported in Table 2.

All the hydrogels showed G′ value greater than G″ value at all frequencies, according to the typical "gel-like" behavior [16]. Consequently, all of them behave as covalently crosslinked networks confirming the infrared spectroscopy results. This behavior is the most suitable for vitreous substitution [2]. In fact, the vitreous should be considered as a slightly gel rather than an entanglement gel or a solution [17]. The average steady state moduli for

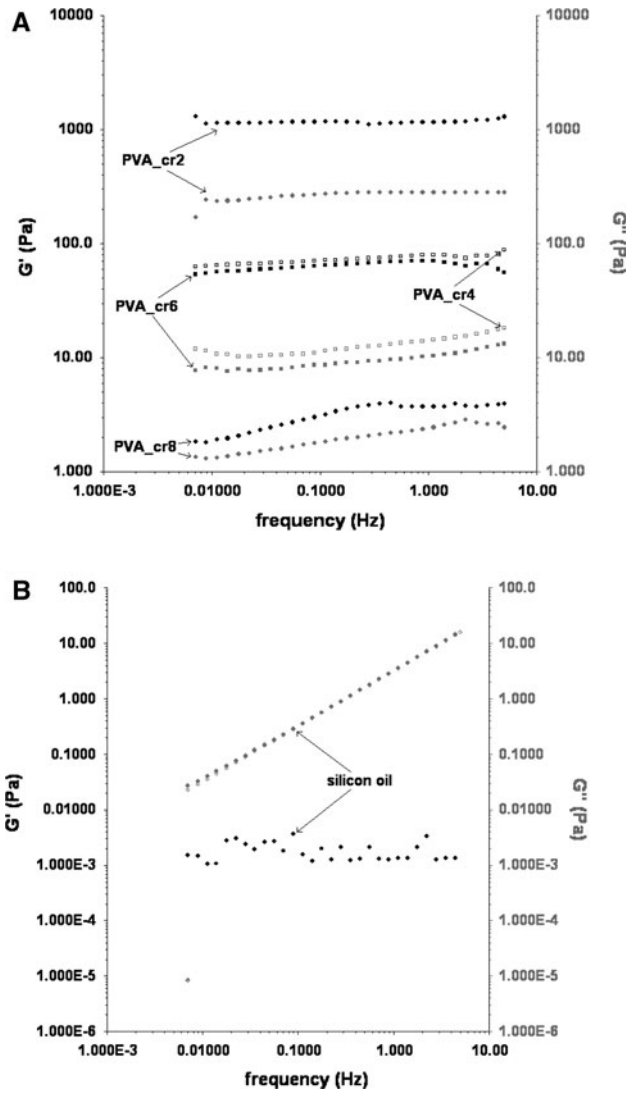

Fig. 2 **a** Storage (G′) and loss (G″) moduli plotted logarithmically against frequency (0.007–5 Hz at 37°C) for fully hydrated PVA_cr2, PVA_cr4, PVA_cr6, PVA_cr8; **b** Storage (G′) and loss (G″) moduli plotted logarithmically against frequency (0.007–5 Hz at 37°C) for a commercial silicon oil used as vitreous temporary substitute

Table 2 Storage and loss moduli of fully hydrated (NaCl 0.9%) PVA_cr2, PVA_cr4, PVA_cr6, PVA_cr8 at 5 Hz compared with bovine vitreous, porcine vitreous and a commercial silicon oil

	G′ (Pa)	G″ (Pa)
Bovine vitreous[a]	7 ± 2	2.2 ± 0.6
Porcine vitreous[a]	2.8 ± 0.9	0.7 ± 0.4
Commercial silicon oil	0.0013 ± 0.0005	14 ± 2
PVA_cr2	1290 ± 64	279.5 ± 13.9
PVA_cr4	78.1 ± 3.9	18.1 ± 0.91
PVA_cr6	20.5 ± 1.1	12.3 ± 0.6
PVA_cr8	3.9 ± 0.1	2.8 ± 0.1

[a] Average steady-state moduli [19]

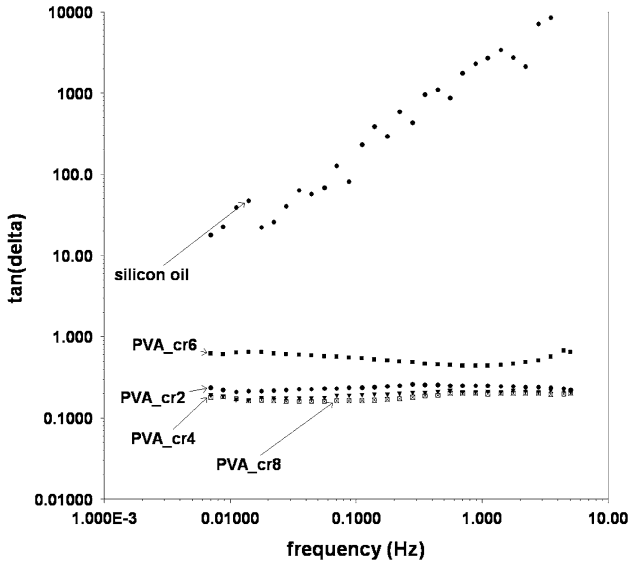

Fig. 3 Loss tangent plotted logarithmically against frequency (0.007–5 Hz at 37°C) for the PVA_cr2, PVA_cr4, PVA_cr6, PVA_cr8 hydrogels and for a commercial silicon oil used as vitreous temporary substitute

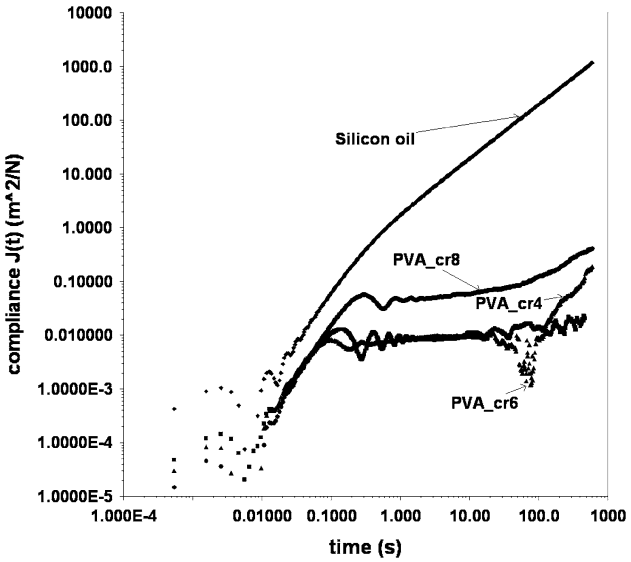

Fig. 4 Creep compliance plotted logarithmically against time for the PVA_cr4, PVa_cr6, PVA_cr8 hydrogels and for a commercial silicon oil used as vitreous temporary substitute

bovine vitreous are $G' = 7 \pm 2$ Pa (mean ± SD) and $G'' = 2.2 \pm 0.6$ Pa whereas for porcine vitreous $G' = 2.8 \pm 0.9$ Pa (mean ± SD) and $G'' = 0.7 \pm 0.4$ Pa. The porcine values resemble the human values [19]. On the contrary, silicon oil appears as a viscous solution with G'' greater than G' for all the frequencies analysed.

The PVA_cr2 can be eliminated for further analysis since its rheological parameters are too high in comparison with porcine rheological parameters.

In Fig. 3 the phase shifts curves relative to all the samples are reported. The lower the loss tangent the higher the resilience [2]. A material with high resilience may perform better mechanically in a vitreous cavity. Therefore the PVA_cr8, and PVA_cr4 should be the best candidates among all the others.

3.2.2 Shearing creep analysis

Representative plots of the creep compliance are shown in Fig. 4.

In his work, Ferry gave a classification of polymers based on their viscoelastic behaviour and in particular on the base of different J(t) logarithmic plots [25].

The compliance of the three analysed hydrogels increases initially and tends to level off to approach a plateau compliance at intermediates times. Accordingly, the creep behaviour of these hydrogels resembles that of 'lightly crosslinked amorphous polymers' defined by Ferry. This confirms the IR spectroscopy and oscillatory shear stress results.

On the basis of this behaviour we can say that there are prominent instantaneous elastic responses followed by substantial retarded elastic responses during the time under constant shear stress.

As widely reported in literature the instantaneous elastic response is mainly because of an increase in internal energy, probably associated with crosslinking points. In this region, the conformational rearrangements of chain backbones is almost immobilised during experiment. On the contrary, the retarded elastic response can be due to the gradual curling and uncurling of randomly entangled polymer chains [26].

The creep plot of silicon oil shows that the compliance curve approaches a horizontal line independent of time. There were no instantaneous or retarded elastic response observable. The material hence exhibits Newtonian flow. Its compliance which may be due to viscous flow, increases with no limit during the duration of the experiment. This sample may be related to type I defined by Ferry [25] as "dilute polymer solution" in which viscoelasticity does not perturb a Newtonian flow greatly [2].

The rheological analysis in terms of G' G'' loss tangent and creep behaviour permitted to identify, among the synthesised hydrogels, PVA_cr8 as the best candidate as vitreous substitutes with a rheological behaviour significantly better than the commercial silicon oil comparing them with porcine vitreous.

3.3 Kinetics of hydration and water uptake

As widely reported, the main component of vitreous is water, which represents up to 99% of vitreous mass. The PVA_cr4, PVA_cr6 and PVA_cr8 samples showed similar

Table 3 Water up-take (obtained as reported in Sect. 2.2.2.3) and Water content (obtained as reported in Sect. 2.2.2.3) of PVA_cr4, PVA_cr6 and PVA_cr8 after 48 h in NaCl 0.9%

	PVA_cr4	PVA _cr6	PVA_cr8
Water uptake [(mg/mg * 100)]	1386 ± 12	1538 ± 24	2486 ± 41
Water content (%)	93 ± 2	94 ± 1	96 ± 1

swelling kinetics reaching the swelling equilibrium after 48 h. All the hydrogels showed a water content value comparable to that of human vitreous, or it is in the range 90–96% (Table 3).

Water content in PVA:STMP hydrogels was affected by the concentration of STMP. In fact, it increases with the decrease of crosslinking agent amount. A less crosslinked matrix is able to absorb a large amount of water. In particular, it is worth to note that the water content of PVA_cr8 hydrogel is close to that of human natural vitreous (99%) [1], so that it could meet the requirement for the water content as artificial vitreous.

3.4 Light transmittance

The results of UV–vis spectrophotometer are listed in Table 4. Decreasing the hydrogel crosslinking degree a softer matrix is obtained having a higher water content and both these aspects permitted a higher light transmittance. The visible light transmission of the only PVA_cr8 hydrogel was more than 85%. That is, it was the only transparent hydrogel and, consequently, still suitable for the realisation of ophthalmic devices [20].

3.5 Cytotoxicity, cell proliferation

PVA_cr4, PVA _cr6 and PVA_cr8 hydrogels were tested for their potential cytotoxic effect and influence towards cell growth on tumoral mouse fibroblasts. As shown by the results reported in Fig. 5 all the tested samples (PVA_cr4, PVA_cr 6, PVA_cr8) were not cytotoxic for mouse fibroblast and they did not interfere with cell growth. In fact, the number of adhered cells/mm^2 in contact with the hydrogels was not statistically different in comparison with the negative control (high density polyethylene). Looking at graph reported in Fig. 5, a slightly not statistically significant difference among cell number in contact with the three hydrogels was revealed. The number of cells in contact with PVA_cr8 was the highest and it decreased in PVA_cr6 and PVA_cr4. This trend may be due to the different mechanical properties of the hydrogels. In fact, the PVA_cr8 being less compact in comparison with the other two hydrogels allows an easier exchange of gases and nutrients and promotes a higher cell growth.

Anyway, as demonstrated by optical microscopy images (Fig. 6) not morphology differences were found between cells in contact with control (Fig. 6a) and those in contact with the hydrogels (Fig. 6b–d). The only difference found was the density of adhered cells whose trend was in accordance with data reported in Fig. 5.

Table 4 Percentage of visible light transmittance in the 380–700 nm wavelength region

	Transmittance (%)
PVA_cr4	80 ± 2
PVA_cr6	83 ± 1
PVA_cr8	94 ± 3

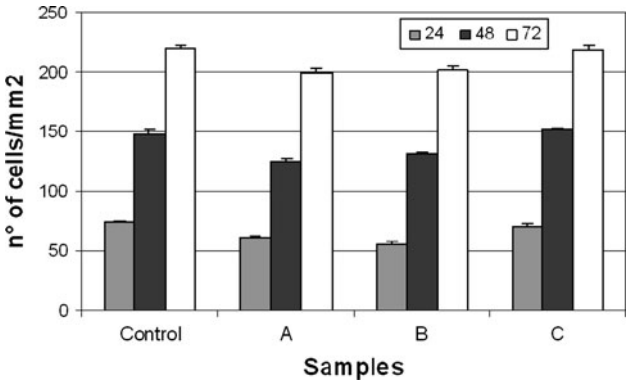

Fig. 5 Fibroblasts NIH3T3 growth in contact with: Control = High Density Polyethylene; A = PVA_cr4; B = PVA_cr6, C = PVA_cr8. Data are means ± standard error of three experiments run in triplicate. No value is statistically significant vs. Control at the same time point

3.5.1 Cell viability

Mouse fibroblasts NIH3T3 viability in contact with the hydrogels was determined for three days at intervals of

Table 5 Number of viable cells in contact with the three different hydrogels as a function of incubation time evaluated by WST-1 assay

Incubation time (h)	Control (no. of viable cells × 10^3 ± SE)	PVA_cr4 (no. of viable cells × 10^3 ± SE)	PVA_cr6 (no. of viable cells × 10^3 ± SE)	PVA_cr8 (no. of viable cells × 10^3 ± SE)
24	1.51 ± 0.13	1.11 ± 0.14	1.27 ± 0.11	1.54 ± 0.12
48	3.12 ± 0.12	2.87 ± 0.11	2.99 ± 0.15	3.18 ± 0.13
72	5.01 ± 0.18	4.53 ± 0.14	4.75 ± 0.10	5.15 ± 0.10

Data are means ± standard error of three experiments run in triplicate. No value is statistically significant vs. Control at the same time point

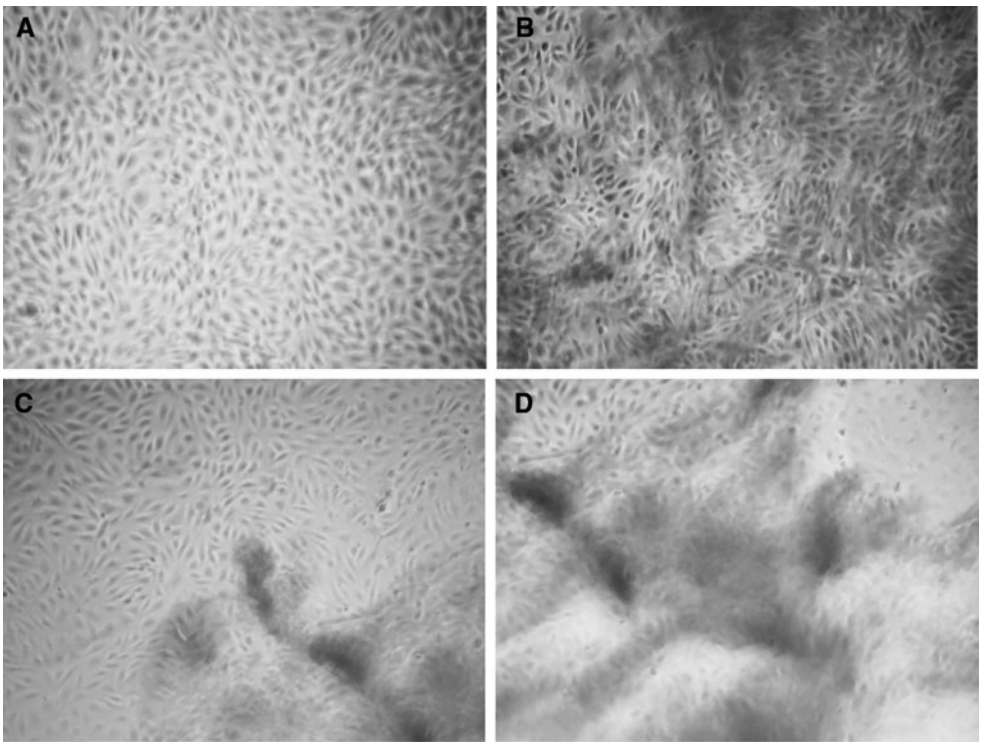

Fig. 6 Optical microscopy images of NIH3T3 fibroblasts after 72 h of contact with **a** Control: High Density Polyethylene; **b** PVA_cr8; **c** PVA_cr6; **d** PVA_cr4. Magnification 20×

24 h by WST-1 assay. The results obtained, reported in Table 5, demonstrated that the mitochondrial activity of fibroblasts after 24, 48 and 72 h of contact with the three different substrates, showed the same characteristics. No impairment of the mitochondrial function or sign of cytotoxicity was found in the cell line. Moreover, the results obtained by WST-1 assay showed the same proliferation trend determined by optical microscopy cell count.

3.6 Thixotropic properties

On the basis of the water content, light transmittance and rheological behaviour, the unique hydrogel suitable as vitreous substitute was PVA_cr8.

PVA_cr8 showed a thixotropic behaviour (Fig. 7). In fact, a perfect overlapping of both G′ and G″ was recorded in the loop test. At a stress value of 80 Pa PVA_cr8 loses its hydrogel consistence showing G″ greater than G′, decreasing the stress, PVA_cr8 recovered its hydrogel consistence.

In Fig. 8 the mechanical spectrum of PVA_cr8 hydrogel after injection through the 19 gauge needle was reported. The injection did not affect the crosslinked structure of the hydrogel. In fact, G′ was higher than G″ after the injection. At a frequency of 5 Hz, a negligible decrease of G′ and increase of G″ was observed. G′ decreased from 3.9 ± 0.2 to 3.5 ± 0.1 Pa and G″ increased from 2.8 ± 0.1 to 3.1 ± 0.1 Pa.

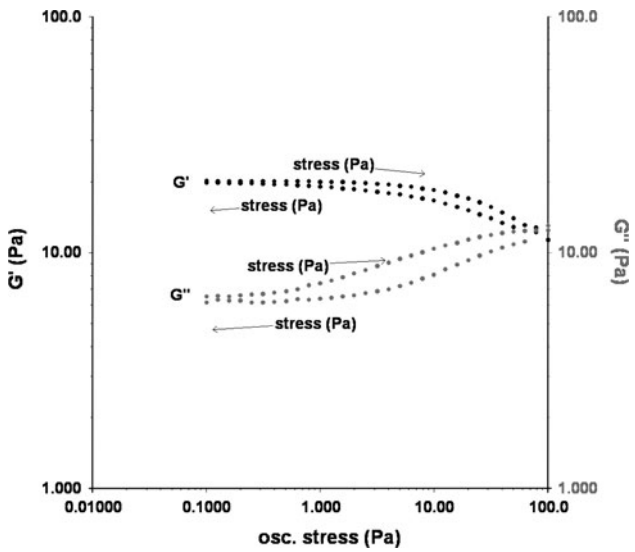

Fig. 7 Storage (G′) and loss (G″) moduli trend of PVA_cr8 as a function of increasing and decreasing stress

The higher amount of water acts as a cushioning and lubricating medium permitting to the crosslinked chains to reorganize them without undergoing significant rupture of the structure [27]. The decrease of G′ or loss of elasticity

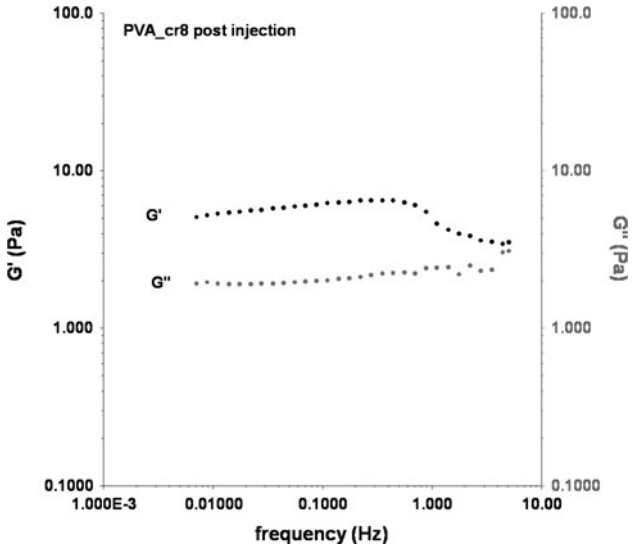

Fig. 8 Storage (G′) and loss (G″) moduli of PVA_cr8 hydrogel determined at 37°C in the frequency range 0.007–5 Hz after the passage through the 19 gauge needle

and the increase of G″ was due to the negligible breakage of crosslinking points [2].

3.7 Diffusion coefficient

The diffusion coefficient of phenylalanine in D_2O was 8.322×10^{-10} m^2/s whereas inside the PVA_cr8 was 8.255×10^{-10} m^2/s. Only negligible decrease of the diffusion coefficient was observed, pointing out an optimal diffusion of solutes through the hydrogel. PVA_cr8 satisfied this fundamental requirement for the foreseen application as vitreous substitute [2, 28].

4 Conclusions

The natural vitreous body in the vertebrate eye has viscoelastic properties. Based on the assumption that any materials to substitute the vitreous should also be viscoelastic, hydrogels with very high water content were obtained by crosslinking PVA with STMP. Five different molar ratios were used to obtain a series of hydrogels with decreasing mechanical properties to realise a material which could be used as potential vitreous substitute. The rheological analysis, the water content determination, the light transmittance measurements and the cytotoxicity test pointed out that among the synthesised hydrogels the PVA_cr8 was able to fulfil the requirements for a good vitreous substitute. Consequently, PVA_cr8 was further characterised in terms of thixotropic behaviour, injectability and permeability. The hydrogel showed good injectability with a negligible change of its rheological properties. Finally, the diffusion coefficient (DC) of a model molecule (phenylalanine) through PVA_cr8 hydrogel is very similar to its DC in water.

These preliminary results suggest that an application as vitreous substitute can be foreseen for PVA_cr8 hydrogel. Further analysis of long term biocompatibility is actually under study.

Acknowledgments The Italian Interuniversity Consortium CSGI supported the research. The authors would like to thank Dr. Renzo Pepi and TA Instruments for putting the AR2000 rheometer at authors' disposal.

References

1. Chirila TV, Hong YE, Dalton PD, Constable IJ, Refojo MF. The use of hydrophilic polymers as artificial vitreous. Prog Polym Sci. 1998;23:475–508.
2. Chirila TV, Hong YE. Poly(1-vinyl-2-pyrrolidinone) hydrogels as vitreous substitutes: a rheological study. Pol Int. 1998;46:183–95.
3. Liesegang TJ. Viscoelastics. Int Ophthalmol Clin. 1993;33:127–47.
4. Fernandez-Vigo J, Refojo MF, Verstraeten T. Evaluation of a viscoelastic solution of hydroxypropyl methylcellulose as a potential vitreous substitute. Retina. 1990;10:148–52.
5. Lloyd AW, Faragher RGA, Denyer SP. Ocular biomaterials and implants. Biomaterials. 2001;22:769–85.
6. Mukai N, Lee PF, Oguri M, Schepens CL. A longterm evaluation of silicone retinopathy in monkeys. Can J Ophthalmol. 1975;10:391–402.
7. Sugar HS, Okamura ID. Intravitreal silicone injection. Arch Ophthalmol. 1976;94:612–5.
8. Eckardt C, Nicolai U, Czank M, Schmidt D. Identification of silicone oil in the retina after intravitreal injection. Retina. 1992;12:17–22.
9. Kirchhof B, Tavakolian U, Paulmann H, Heimann K. Histopathological findings in eyes after silicone oil injection. Graefe's Arch Clin Exp Ophthalmol. 1986;224:34–7.
10. Budde M, Cursifen C, Holbach LM, Naumann GOH. Silicone oil-associated optic nerve degeneration. Am J Ophthalmol. 2001;131:392–4.
11. Couplaud SE, Heimann H, Lee WR. Histopathological changes on ocular tissues following silicone oil tamponade in vitreoretinal surgery. In: Kriegelstein GK, editor. Retinology today (In Memoriam Klaus Heimann). Gemmering: Ad manum medici; 2000. p. 37–42.
12. Eller AW, Friberg TR, Mah F. Migration of silicone oil into the brain: a complication of intraocular silicone oil for retinal tamponade. Am J Ophthalmol. 2000;129:685–8.
13. Capone JA, Aaberg TM. Silicone oil in vitreoretinal surgery. Curr Opin Ophthalmol. 1995;6:33–7.
14. Yamauchi A, Matsuzawa Y, Nishioka K, Hara Y, Kamiya S. PVA hydrogel for vitreous replacement. Kobunshi Ronbunshu. 1977;34:261–6.
15. Gliko-Kabir I, Penhasi A, Rubinstein A. Phosphated crosslinked guar for colon-specific drug delivery I Preparation and physicochemical characterization. J Controll Rel. 2000;63:121–7.
16. Ross-Murphy SB. Rheological characterization of polymeric gels and networks. Polym Gel Netw. 1994;2:229–37.
17. Dalton DP, Chirila TV, Hong Y, Jefferson A. Oscillatory shear experiments as a criteria for potential vitreous substitutes. Polym Gel Netw. 1995;3:429–44.

18. Van Krevelen DW. Properties of polymers. 3rd ed. Amsterdam, The Netherlands: Elsevier; 1990. p. 388–411.
19. Nickerson CS, Park J, Kornfield JA, Karageozian H. Rheological properties of the vitreous and the role of hyaluronic acid. J Biomech. 2008;41:1840–6.
20. Lin CH, Lin WC, Yang MC. Fabrication and characterization of ophthalmically compatible hydrogels composed of poly(dimethyl siloxane-urethane)/Pluronic F127. Colloids Surf B Biointerfaces. 2009;71:36–44.
21. Barnes HA. Thixotropy—a review. J Non-Newtonian Fluid Mech. 1997;70:1–33.
22. Stejskal EO, Tanner JE. Spin diffusion measurements: spin echoes in the presence of a time dependent field gradient. J Chem Phys. 1965;42:288–92.
23. Liu M, Mao X, Ye C, Nicholson JK, Lindon JC. Improved WATERGATE pulse sequences for solvent suppression in NMR spectroscopy. J Magn Reson. 1998;132:125–9.
24. Bellamy LJ. The infrared spectra of complex molecules. 2nd ed. London: Chapman and Hall Ltd; 1980.
25. Ferry JD. Viscoelastic properties of polymers. 3rd ed. New York USA: John Wiley & Sons; 1980. p. 34–40.
26. Leaderman H. In: Eirich FR, editor. Rheology: theory and applications, vol. II. New York, USA: Academic Press; 1958. p. 1–61.
27. Barbucci R, Leone G, Lamponi S. Thixotropy property of hydrogels to evaluate the cell growing on the inside of the material bulk (Amber Effect). J Biomed Mater Res B Appl Biomater. 2006;76B:33–40.
28. Matsuyama H, Teramoto M, Urano H. Analysis of solute diffusion in poly(vinyl alcohol) hydrogel membrane. J Membr Sci. 1997;126:151–60.